JOURNAL OF BACTERIOLOGY, Mar. 1972, p 1221-1231

Vol. 109, No. 3
Printed in U.S.A.

Morphokinetic Reaction of Cells of *Streptococcus faecalis* (ATCC 9790) to Specific Inhibition of Macromolecular Synthesis: Dependence of Mesosome Growth on Deoxyribonucleic Acid Synthesis

MICHAEL L. HIGGINS AND LOLITA DANEO-MOORE

Department of Microbiology and Immunology, Temple University School of Medicine, Philadelphia, Pennsylvania 19140

Received for publication 4 October 1971

The application of quantitative electron microscopy to thin sections of cells of *Streptococcus faecalis* specifically inhibited for deoxyribonucleic acid (DNA), ribonucleic acid, and protein synthesis shows that septal mesosomes (i) increase in size when protein synthesis is inhibited by at least 80% while DNA synthesis proceeds at no less than 50% of the control rate and (ii) decrease in size when DNA synthesis is inhibited 50% or more during the initial 10 min of treatment. This indicates that fluctuations in mesosome size are dependent on the extent of DNA synthesis. The fluctuations in mesosome areas observed on treatment do not correlate with the kinetics of glycerol incorporation per milliliter of a culture. However, when glycerol incorporation is placed on a per cell basis, a strong correlation is observed between increases in (i) the thickness of the electron-transparent layer of the cytoplasmic membrane and (ii) the amount of glycerol incorporated per cell. It seems that the electron-transparent membrane layer may thicken to accommodate changes in lipid content when protein and lipid synthesis are uncoupled.

Morphologists and biochemists have sought a membranous organelle directly involved in prokaryotic deoxyribonucleic acid (DNA) synthesis. Thin sections of dividing bacteria consistently have shown nuclear fibrils to be intimately associated with the mesosomes or internal membranes of many gram-positive bacteria (14). Based on these morphological associations, many workers have considered that mesosomes or membrane-DNA attachment points may play a functional role in chromosome replication or segregation, or both (9, 14).

The isolation of the DNA replication point associated with a rapidly sedimenting structure, possibly membrane (3, 4, 16), and a different attachment point associated with the origin and possibly the terminus (2, 17) of the chromosome has given added credibility to past morphological observations and projections. Recently, in a strain of *Escherichia coli* that forms intracytoplasmic membranes at elevated temperature, autoradiography was used to show the location of pulse-labeled DNA (1). Twenty-four per cent of the membrane-DNA complexes observed in sections produced grains, as opposed to 7% producing grains after a 20-min chase, suggesting that the replication fork may be associated with the intracytoplasmic membranes. However, we are not aware of any direct information that relates mesosome formation and growth to actual DNA synthesis. We show by selective inhibition of macromolecular synthesis [DNA, ribonucleic acid (RNA), and protein] coordinated with quantitative electron microscopy that DNA synthesis is necessary for mesosome growth.

MATERIALS AND METHODS

Fixation and embedding. The conditions of the glutaraldehyde-osmium tetroxide fixation, Epon 812 embedding, and uranyl acetate-lead citrate staining have been given elsewhere (7).

Determination of mesosomal area. The proce-

dure for measuring the mesosomal area in a given longitudinal central cell section has been described previously (7). Briefly, the procedure entails directly superimposing a grid pattern contained in the eyepiece of a Bausch & Lomb dissection microscope upon a well focused electron image plate at ×7 magnification (taken at about ×30,000 with a microscope calibrated daily with a carbon-grating replica). In using this technique, it is important that only cells showing tribanded wall around the entire cell perimeter be used, because the reconstruction of serial sections has shown that a complete tribanded profile can be produced only when the section is closely aligned to the longitudinal axis and passes through the central 15 to 25% portion of the cell (7). These conclusions are based on observations that 13 to 14 longitudinal sections are required to transverse the cell and that, of these, only the central 2 to 3 sections yield a complete tribanded wall margin. Also, when the plane of the section is not closely parallel to the longitudinal axis of the cell, a tribanded wall around the entire cell is not observed, and a diffuse wall outline is seen.

For quantitative purposes, a coccus in the process of dividing was considered to be two daughter cells (A and B in Fig. 1), based on the observation of a nascent cross wall in a cell where septation from the previous generation was complete. To convert the average mesosomal area per daughter cell to a per cell basis, the average daughter cell figure was multiplied by two.

Serial sections have also shown that cross wall formation is always preceded by the formation of a single equatorial mesosome and that the body of the mesosome appears to grow rapidly into one daughter cell or the other (7, 8). This pattern of mesosome growth is reflected by observations of random, central, longitudinal cell sections, where a portion of the body of a mesosome is seen in 38 ± 5% of the daughter cells and 75 ± 4% of the cells. Deviation from these daughter cell and whole cell frequencies upon treatment would indicate a deviation from the average number of mesosomes per exponential-phase cell.

The cytological effect of each treatment was quantitated in at least two separate experiments, and every experimental point required the analysis of at least 40 cells, usually by two workers.

Determination of membrane thickness. A thin section passing through an isolated membrane in an antitangential manner produces a typical electron-dense-transparent-dense profile. The thickness of the transparent middle layer (M2 in Fig. 2) is readily determined. However, measurement of the thickness of the two dense layers is complicated in sections of whole cells of *Streptococcus faecalis* in that (i) the outer electron-dense layer (M1 in Fig. 2) is commonly opposed to the inner layer of the cell wall and (ii) the inner electron-dense membrane layer blends into the cytoplasm and cannot be defined for measurement (7). It is possible to measure the outer dense layer (M1) by finding areas where it is distinguishable from the cell wall (Fig. 2), but no method has been developed to measure the thickness of the inner dense layer.

The thickness of the membrane layers (M1 and M2 in Fig. 2) was evaluated directly from the electron microscope plates by using an eyepiece microm-

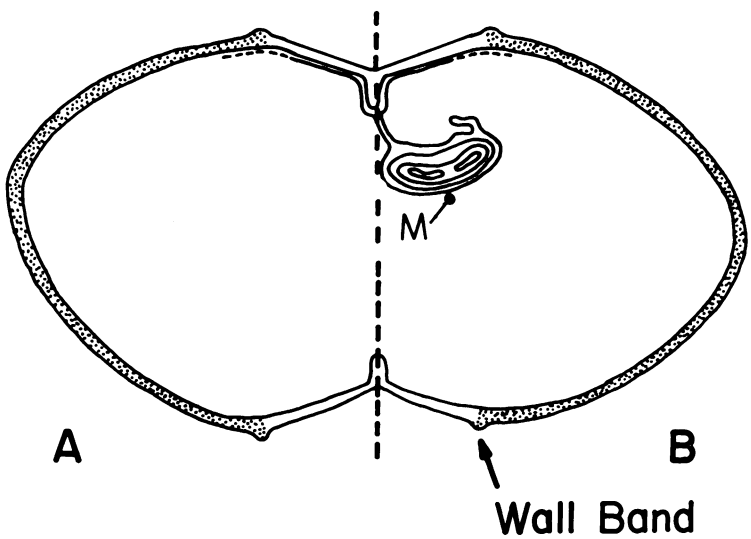

FIG. 1. *Diagrammatic representation of a central longitudinal section of a typical exponential-phase cell. The mesosome (M) of this organism is a bag-shaped organelle connected to the septal membrane by a thin stalk (7, 8). For purposes of quantitating the mesosomal area per section, a cell showing a cross wall was divided into two daughter cells, A and B. Only cells showing a tribanded wall profile around the entire daughter cell were measured. The amount of mesosomal area was obtained by a grid-overlay technique described in the text. The protuberances on the external portions of the cell wall are known as wall bands and appear to act as lines of demarcation between old polar wall and new equatorial wall (6, 8).*

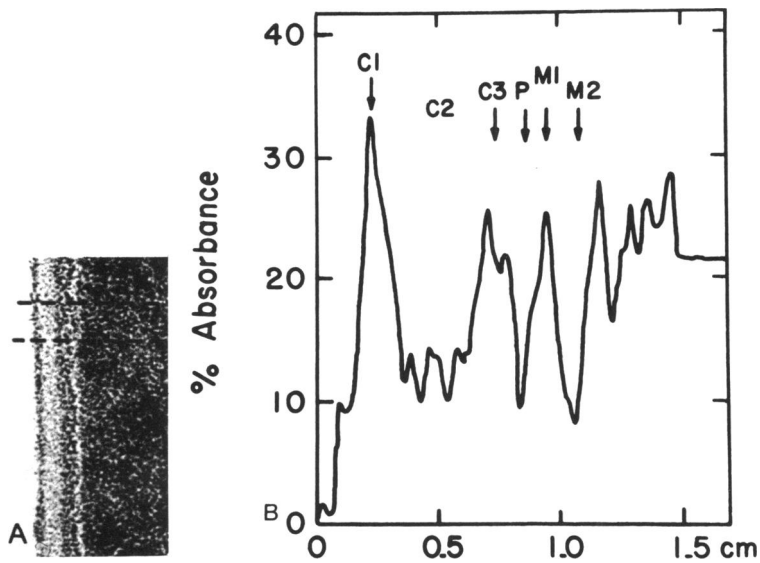

FIG. 2. *Density scan of a thin-sectioned cell envelope profile. The two parallel lines in the electron micrograph (A) indicate the area of envelope scanned. The densitometer tracing (B) (obtained with a Gilford 2,000 spectrophotometer equipped with a linear absorbance readout) shows a tribanded dark (C1)- light (C2)- dark (C3) cell wall followed by a periplasmic space (P), and finally concluded with the outer dark (M1) and the middle transparent (M2) layers of the membrane. The third dense layer of membrane cannot be seen because of the density of the cytoplasm.*

eter (10-mm scale in 0.1-mm divisions) fitted in a Bausch & Lomb dissection microscope at ×30 magnification. Two measurements were taken from at least 40 cells on at least 2 separate days.

The screening and determination of antibiotic level. Antibiotics were screened by addition to cultures of constant mass (340 OD_{675} units = 136 μg/ml). Each antibiotic was examined at various concentrations for effects on culture mass. A narrower range of concentrations was then used to determine effects on cellular DNA, RNA, and protein synthesis and on the incorporation of glycerol into trichloroacetic acid-precipitable material. For incorporation studies, the cultures were prelabeled for 6 to 10 mass doublings as described previously (13). The threonine starvation procedure has been described before (7, 19).

The data obtained from incorporation studies of treated cells are expressed as per cent of control synthesis. All incorporation values were related to amount incorporated at the time of antibiotic addition, which was given a relative value of 1.0. Consequently, in a control culture with a doubling time of 30 min, the amount incorporated at 30 min would be 2.0. A treated culture with a relative incorporation value of 1.75 would be considered at 30 min to have synthesized [(1.75-1.0)/(2.0-1.0)] × 100, or 75% of the amount incorporated by the control culture.

The increase in cell numbers after treatment. After various times, untreated controls and antibiotic-treated cultures were chilled in a final concentration of 10% Formalin for 1 hr, diluted to 0.08 to 0.24 μg of bacterial substance per ml in isotonic saline, and counted as soon as possible in a model B Coulter counter equipped with a 30-μm orifice (18).

RESULTS

Previous quantitative electron microscope studies on *S. faecalis* showed that, during the initial 60 min of either threonine or valine starvation, there was a relatively rapid increase in mesosomal area (7). Since it was known that during this period of amino acid starvation there is little or no RNA or protein synthesis occurring (21), it was postulated that the observed increase in mesosomal membrane might be related to the continued poststarvation synthesis of DNA commonly observed in a large number of microorganisms after the inhibition of protein synthesis.

To test this hypothesis, antibiotics were used to inhibit specifically DNA, RNA, and protein synthesis. The kinetics and degree of inhibition of synthesis of the various macromolecules were then correlated with the observed mean mesosomal area per central cell section.

Specific inhibition of macromolecular synthesis. A large number of antibiotics at various concentrations were screened for their ability to inhibit specifically the synthesis of

DNA, RNA, or protein. The specificity of inhibition was determined by noting the effect of antibiotic addition on the incorporation of fully equilibrated, specific labels of protein (^{3}H- or ^{14}C-leucine), RNA (^{3}H- or ^{14}C-uracil), or DNA (^{3}H- or ^{14}C-thymidine) into acid-precipitable material. Based upon incorporation studies, five antibiotics (chloramphenicol, 50 μg/ml; 5-azacytidine, 5 μg/ml; rifampin, 0.1 μg/ml; actinomycin D, 0.25 μg/ml; and mitomycin C, 0.5 μg/ml) plus threonine starvation were selected for study. Inhibition of RNA, DNA, and protein synthesis, expressed as per cent of incorporation of the control culture, is given in Fig. 3. Collectively these data indicate that specific inhibition of DNA, RNA, and protein synthesis by antibiotics is a relative phenomenon which is usually observed only within the first 30 min of treatment. Considering this initial 30 min of exposure, chloramphenicol and 5-azacytidine appeared to be fairly specific inhibitors of protein synthesis. Threonine starvation, operating through a stringent control mechanism (21), was shown to inhibit RNA as well as protein synthesis, and mitomycin C appeared to result in a relatively specific inhibition of DNA synthesis. Rifampin and actinomycin D showed the least specificity. After 30 min of treatment, both drugs inhibited protein and RNA synthesis over 90%; DNA synthesis was also markedly inhibited (50% or more). The inhibition of protein synthesis by 5-azacytidine was observed to be a competitive phenomenon and was therefore concentration-dependent. After 30 min of treatment, the inhibition was slowly reversed.

Effect of specific inhibition of macromolecular synthesis on mesosome area. The changes in mesosome area were compared to the reduction in amounts of DNA, RNA, and protein synthesized after the various treatments (Fig. 3). The dashed line in the mesosome plots indicates the average mesosomal area per central cell section of a culture dividing every 31 to 33 min (i.e., 7.3×10^3 to 9.4×10^3 nm^2 per daughter cell, or 14.6×10^3 to 18.8×10^3 nm^2 per cell). In each experiment, the control area was given a relative area of 1.0. Values falling above or below this base line indicate increases or decreases in mesosome size with respect to the average control value for the individual experiment. Mesosome areas increase over the control value in cells where residual DNA synthesis is proceeding at a rate 50% or more of that of the control synthesis, while at the same time protein synthesis is inhibited 80% or more. It therefore seems that the greatest and fastest increase in mesosomal area appears when DNA synthesis experiences the least inhibition and when protein synthesis experiences the greatest inhibition. The inhibition of RNA synthesis appears to be relatively unimportant since increases in mesosomal area were observed in chloramphenicol- and 5-azacytidine-inhibited cultures where, during the early stages, RNA synthesis was virtually unaffected.

Conversely, only a marginally significant increase followed by a decline in area of mesosomal membrane was observed upon treatment with actinomycin, rifampin, or mitomycin, whereas, within the first 10 min, DNA synthesis was inhibited by 50% or more. Thus, rapid inhibition of DNA synthesis appears to prevent an increase in mesosomal area. More complex explanations, such as an antagonistic relationship between DNA synthesis and protein synthesis or DNA synthesis and RNA synthesis are ruled out, since mesosomal membrane declines of the same order of magnitude are observed in cultures where RNA and protein synthesis are inhibited to less than 40% (mitomycin) as well as in cultures where protein and RNA synthesis are essentially nonexistent (actinomycin and rifampin).

Morphology of the mesosome. None of the treatments altered the basic architecture of mesosomes observed in exponential growth (Fig. 4). That is, after all treatments the mesosome appeared to be a bag of membranes attached to the septal membrane by a stalk (Fig. 1 and 4). With time, all treatments resulted in (i) the electron-transparent layer of the mesosomal as well as the cytoplasmic membrane increasing in thickness, (ii) the bag portion of the mesosome becoming less tubular-vesicular and more onion-lamella-like, (iii) a slight increase in the number of observed mesosomes attached to the poles of the cells, and (iv) an increasing tendency to observe small, vesicular-shaped membranes associated with the perimeter of the cell (7). The small vesicular membranes and polarly attached mesosomes in no case contributed more than 5% of the total mesosomal area and were usually observed only after 30 min or more of treatment. However, more polarly attached mesosomes and much less membrane thickening were observed after mitomycin addition than after any other treatment.

Frequency of observation of mesosomes and distribution of area size classes after treatment. Previous serial section analyses

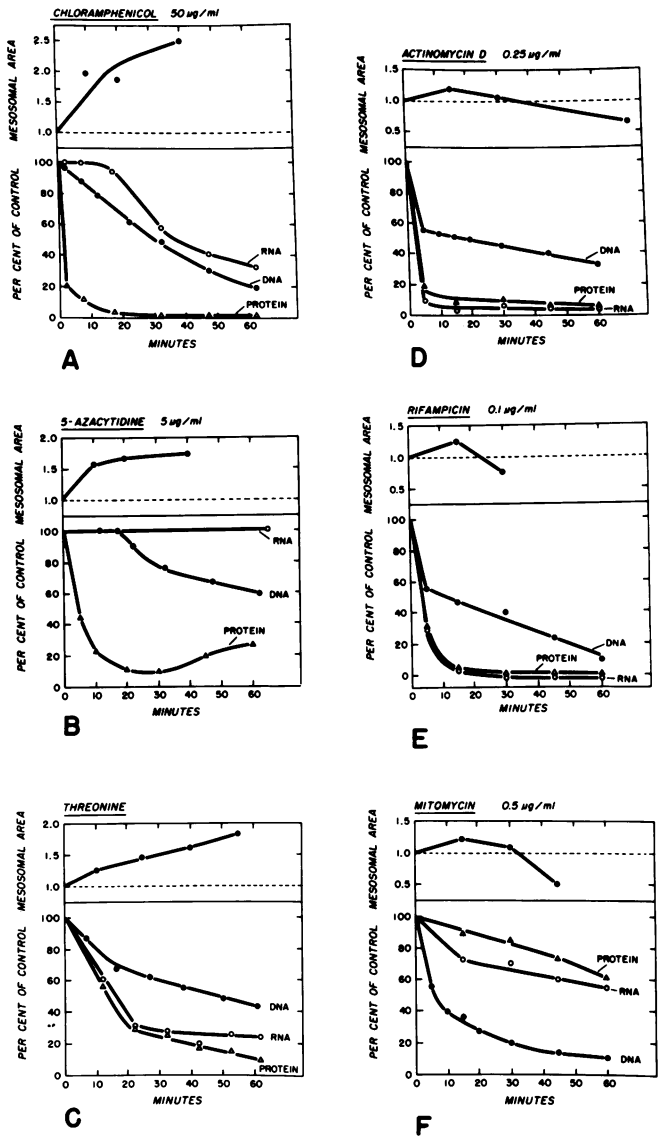

FIG. 3. *Fluctuation of mesosomal pool area per daughter cell after treatment as compared to per cent incorporation of DNA, RNA, and protein with respect to the control values. The dashed base line represents the mean mesosomal area per central cell section of exponential-phase cells (7.3 × 10³ to 9.4 × 10³ nm² per daughter cell and 14.6 × 10³ to 18.8 × 10³ nm² per cell depending on the experiment). The unit 2 along the abscissa of the mesosomal plots indicates the point at which the mesosomal area doubles with respect to the exponential-phase population. Each experimental point resulted from the analysis of at least 40 cells.*

showed that mesosome formation precedes cross wall formation in exponential-phase cultures of *S. faecalis* (7, 8), and that they both are initiated from the same wall band surface site (Fig. 1). A single mesosome appears to be formed by a membranous invagination into the cytoplasm, creating a stalked bag which remains attached to the septum throughout most of the growth cycle (7). After formation, the bag portion appears to grow quickly into one of the daughter cells.

Therefore, serial section studies would indicate that most exponential-phase cells should contain a single septal mesosome with its bag

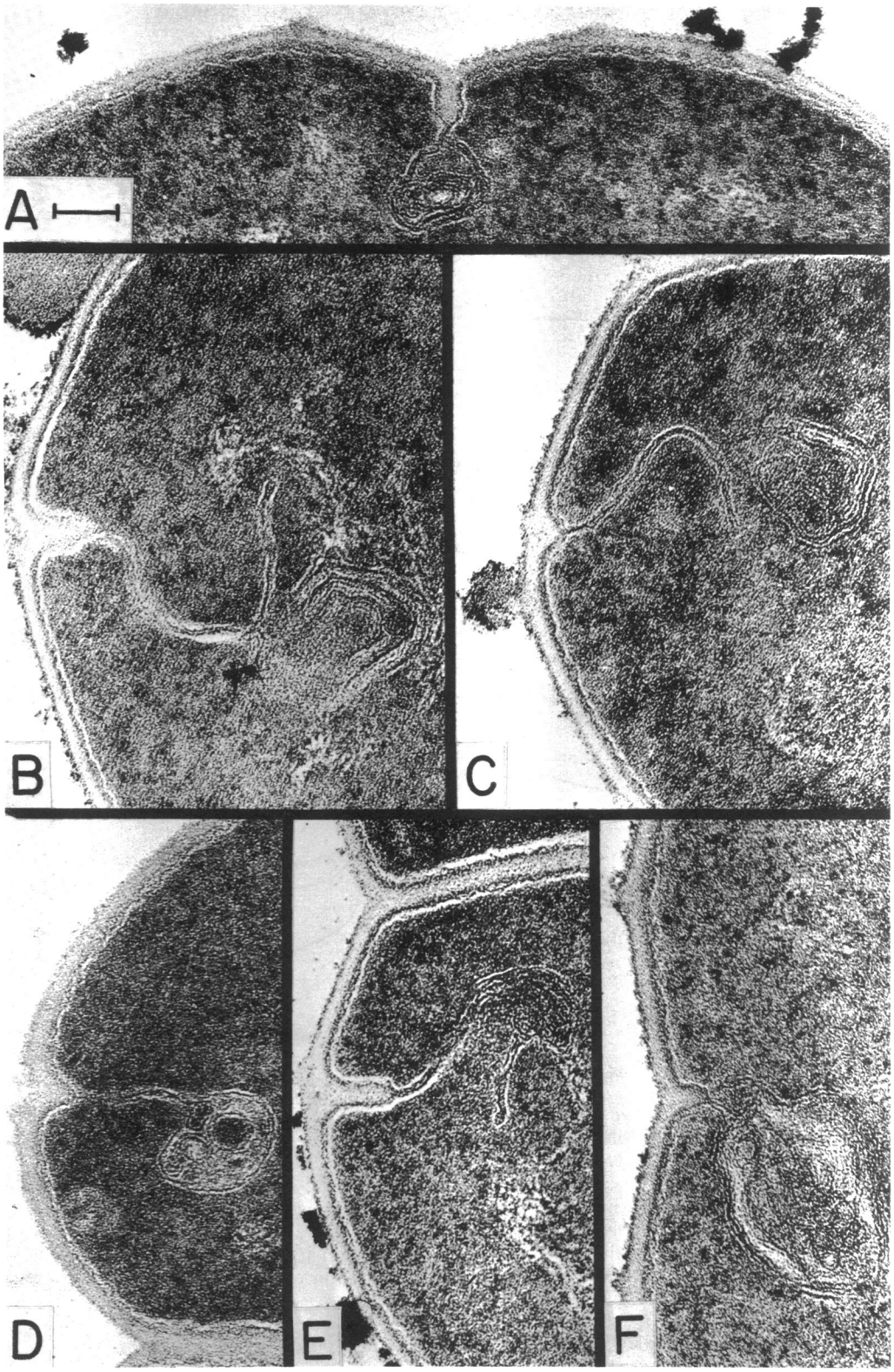

FIG. 4

portion located in one of the daughter cells. Besides reconstructing serial sections, evidence for the general presence of a single asymmetrically located mesosome can also be generated from a random section analysis of the frequency of mesosome observation per daughter cell as compared to the frequency per cell.

In seven separate experiments it was observed that, in balanced exponential-phase cultures dividing every 31 to 33 min, 38 ± 5% of the daughter cell sections and 75 ± 4% of the cell sections contained mesosomes. These frequencies are consistent with the presence in most cells of a single asymmetrically located mesosome, and deviation from these frequencies would suggest a change in the placement or average number of mesosomes per cell.

Upon treatment, the frequencies of mesosome observations per daughter cell section (35 to 42%, Fig. 5) and per cell section (74 to 78%, not shown) remain essentially at the exponential-phase values. These normal cell range frequencies, combined with the observation that the treated mesosomes, like normal mesosomes, are also preponderantly septally attached (Fig. 4), indicate that there is no demonstrable change in the number or attachment of the treated mesosomes. Furthermore, these data suggest that, in antibiotic-treated cells (as in normal cells), a mesosome is produced every time a cross wall is initiated.

Figure 5 also gives a histogram analysis of mesosomal area frequencies from normal and treated populations at selected times. This analysis considers only daughter cells which contain mesosomes. It shows that the average mesosome area increases shortly after chloramphenicol and 5-azacytidine addition and threonine starvation, and decreases after 20 to 30 min of actinomycin, rifampin, or mitomycin addition. These data provide strong evidence that the fluctuations in the average mesosomal areas given in Fig. 3 are in fact a reflection of changes in area of the mesosomes.

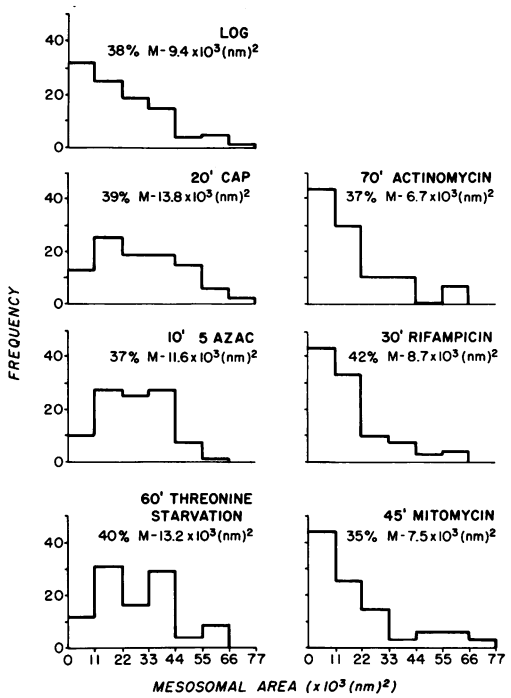

FIG. 5. *Histogram analysis of the frequency of mesosome area from normal and treated daughter populations containing mesosomes. Above each histogram is given the antibiotic, the time in minutes of treatment, the percentage of daughter cell sections containing mesosomes, and the average mesosomal area per daughter cell. (To obtain the mean mesosomal area per cell, multiply by 2.) The distribution of area classes in the exponential-phase population (log) is skewed towards the smaller mesosomes. This skewed distribution is also shown in treatments that result in a net decrease in average mesosomal area with respect to the controls (actinomycin, rifampin, and mitomycin), while those treatments which permit an increase in average mesosomal area (chloramphenicol and 5-azacytidine treatment and threonine starvation) produce a more normal distribution. The concentration of each antibiotic as well as the method for measuring mesosome area is given in the text.*

FIG. 4. *Mesosome structure of normal and treated cells taken from longitudinal sections. The treated cells retained the basic exponential-phase mesosome structure, that is, the bag portion of mesosome was predominantly attached to the septal membrane by a stalk. The micrographs were selected to show the basic structure and attachment of the treated mesosomes and not to reflect their average sizes. The bar in A applies to all figures and represents 100 nm. A is a normal exponential-phase cell, B was treated for 20 min with chloramphenicol, C was treated with 5-azacytidine for 40 min, D was treated 30 min with actinomycin D, E was after 30 min of rifampin, and E was after 45 min of mitomycin C. Pictures of the mesosomes of threonine-starved cells have been presented previously (7). Antibiotic concentrations are given in the text. After treatment with chloramphenicol (B), 5-azacytidine (C), rifampin (D), actinomycin (E), and threonine starvation (not shown here), the middle electron-transparent layer of the cytoplasmic membrane thickened. Only the mitomycin-treated membranes failed to thicken during the initial 30 min of observation. D does not show the marked thickening typically observed in actinomycin-treated cultures since this section, selected to show mesosome structure and attachment, is not a central one as defined in the text.*

The mesosomal pool and glycerol incorporation. There seems to be little correlation between the relative rate of glycerol incorporation into acid-precipitable material (Table 1) and the observed changes in mesosomal areas after antibiotic addition (Table 1 and Fig. 3). For example, after 40 min of chloramphenicol treatment, glycerol incorporation is inhibited approximately 30% (derived from data in Table 1), whereas mesosomal membranes continue to increase in area. On the other hand, in mitomycin-treated cells the average mesosomal area is observed to decrease while glycerol incorporation continues at essentially the control rate.

In spite of the lack of correlation between glycerol incorporation and mesosome size, it was noted in every treatment, except during the initial 30 min of exposure to mitomycin, that the electron-transparent layer of cell membrane increased in thickness with time (Fig. 4B, C, and E). To determine whether the change in membrane thickness could account for the kinetics of glycerol incorporation, the thickness of the outer electron-dense (M1, Fig. 2) and the middle electron-transparent layer (M2, Fig. 2) of cell membrane were measured (Fig. 6). Because of the density of the cytoplasm, the thickness of the inner dense layer could not be measured. The kinetics of membrane thickening were compared to the relative increase in amount of glycerol incorporated per cell (Fig. 6C). This was done by dividing the relative increase in glycerol incorporation by the relative increase in cell numbers after treatment (Table 1). It was observed that blockage of cell division was related to an inhibition of protein synthesis; therefore, significant increases in cell numbers were observed only after 20 min of 5-azacytidine treatment (when the initial inhibition of protein synthesis is slowly reversed) and during the first 30 min of mitomycin C treatment (Table 1).

TABLE 1. *Effect of antibiotic treatment on relative increases in amount of glycerol incorporated and cell numbers with time*

Antibiotic	Time of treatment (min)	Relative increase in amt of glycerol incorporated	Relative increase in cell numbers
Chloramphenicol	15	1.37	1.00
50 μg/ml	30	1.73	1.00
	45	2.10	1.00
	60	2.41	1.00
5-Azacytidine	10	1.30	1.03
5 μg/ml	20	1.56	1.08
	30	1.94	1.25
	40	2.36	1.43
	60	3.50	1.98
Actinomycin D	8	1.36	1.05
0.25 μg/ml	15	1.48	1.10
	30	1.90	1.08
	45	2.22	1.08
	70	2.55	1.10
Rifampin	8	1.26	1.02
0.1 μg/ml	15	1.43	1.05
	30	1.87	1.06
	45	2.20	1.06
	60	2.50	1.09
Mitomycin C	8	1.18	1.21
0.5 μg/ml	15	1.37	1.40
	30	1.70	1.76
	45	2.10	1.76
	60	2.49	1.80

From Figure 6 it seems that the thickness of the electron-dense layer (M1) is little altered by treatment; however, the electron-transparent layer (M2) experiences sizable increases in thickness after most of the treatments. Cell division proceeding in the presence of protein synthesis (after 20 min of 5-azacytidine addition and during the first 30 min of mitomycin treatment) seemed to antagonize membrane thickening, whereas in those cases where protein synthesis and cell division were greatly inhibited (chloramphenicol, actinomycin, and rifampin), the membrane underwent rapid thickening. The kinetics of membrane thickening and glycerol incorporation seem to correlate closely. This correlation is observed even though changes in cell shape were not accounted for in the glycerol incorporation per cell data.

DISCUSSION

Under conditions where protein synthesis was inhibited by more than 80% and DNA synthesis was inhibited by less than 50%, septal mesosomes were observed to increase in area. Conversely, mesosomal membrane accumulation was blocked when DNA synthesis was inhibited by 50% or more within the first 10 min of treatment. The fluctuations in mesosomal area were not due to any apparent variation in the number of mesosomes per cell and seemed to be related to an actual increase or decrease in the size of the mesosomes themselves.

Previous studies have indicated that equatorial mesosomes lose their septal connection before the cross wall is completely closed. The loss of septal connection occurs at about the time that the nuclear figures double in number and two new mesosome-cross wall growth points appear under the wall bands of the

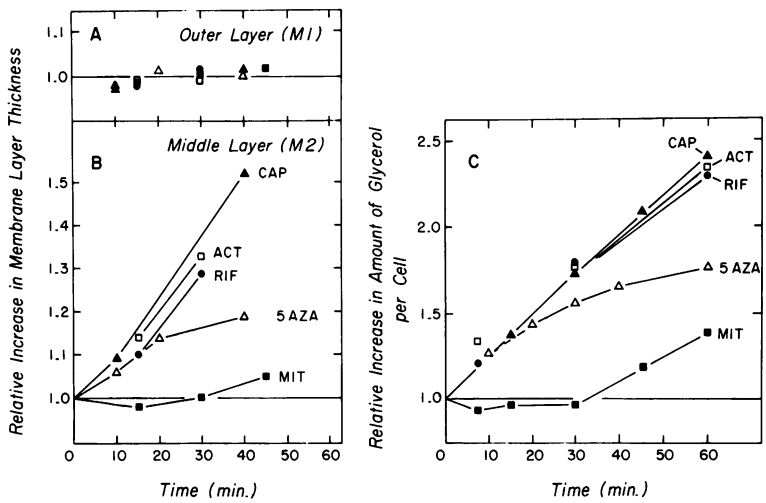

FIG. 6. *Comparison of the effect of antibiotic treatment on the thickness of the outer (M1) electron-dense (A) and the middle (M2) electron-transparent (B) membrane layers, with respect to the relative amount of glycerol incorporated per cell with time (C). The two membrane layers were measured as described in the text. The relative increase in layer thickness was calculated by dividing the mean exponential-phase layer thickness (for M1 4.66 nm, SD = 7.9 nm, and for M2 3.56 nm, SD = 7.9 nm) into the treated thickness. The standard deviations for the outer dense treated layer ranged between 0.58 to 0.92 nm, and the range for the middle transparent treated layer ranged between 0.54 to 0.97 nm. Each experimental point was produced by the measurement of at least 40 cells. The relative increase in amount of glycerol incorporated per milliliter of culture was divided by the relative increase in cell numbers per milliliter after treatment (Table 1).*

daughter cells (Fig. 1; reference 6).

On the basis of when and where the mesosomes appear and disappear in the cell cycle, it was suggested (8) that mesosome formation in *S. faecalis* is more logically related to cross wall initiation and DNA replication than to cross wall growth and completion. This hypothesis seems quite reasonable from recent studies with *E. coli* which suggest that separate DNA membrane associations could be involved in replication and segregation (2). The hypothesis involving mesosome growth and DNA replication appeared to be consistent with the data reported within the body of this paper, which suggests that an increase in mesosome area is related to some continued DNA synthesis. This would be compatible with a model in which, as long as DNA synthesis is occurring within the cell, the bag portion of the mesosome continues to increase in size. The degradation of a mesosome possibly resulting in the release of precursors into a cytoplasmic pool which would be available for reassembly could occur in a normal cell cycle after a round of DNA replication.

If we are observing mesosomal increases in response to the completion of rounds of DNA synthesis, the questions arise (i) why is inhibition of protein synthesis necessary and (ii) why do the mean areas of mesosomes increase above normal values? These questions can best be answered by observing the area frequency distribution of mesosomal membrane (Fig. 5) for exponentially dividing (A), chloramphenicol-treated (B), 5-azacytidine-treated (C), and threonine-starved (D) cells. It is seen that for normal cells the size class distributions are skewed towards the smaller, mesosomal areas. This would be expected since in an exponentially dividing population more cells are starting the cell cycles than finishing them. Therefore, there would be more newer, smaller mesosomes than larger, older mesosomes. On inhibition of protein synthesis by chloramphenicol or 5-azacytidine treatment or threonine starvation, cell division is inhibited (Table 1). This inhibition of protein synthesis and of cell division, in the presence of DNA synthesis, would, according to our model, allow the small mesosomes found in the cells before treatment to grow to full maturation after treatment, while inhibiting the formation of new, small mesosomes.

This interpretation of our results would attempt to identify the mesosomes of this organism as an organelle of DNA replication and possibly cross wall initiation. Thus, other membrane DNA association sites, such as those shown in *E. coli*, involving the origin or possibly the terminus of the chromosome (2,

17), could be involved in the segregation of the nucleoid. After the completion of a round of DNA replication, the segregation membrane-DNA association sites [conceivably associated with the wall band regions of this organism (Fig. 1)] could be activated to form a mesosomal replication site in concert with the initiation of new rounds of DNA synthesis.

It was noted that glycerol incorporation could be related to thickness of the electron-transparent layer of the membrane, but not to mesosomal area increases and decreases in treated cells. Therefore, the electron-transparent layer may be a "breathing layer" which could adjust to changes in membrane lipid-to-protein ratios reported for *S. faecalis* on amino acid starvation and for other organisms on the addition of chloramphenicol (10, 11). This would be analogous to the cell wall thickening mechanism observed in cells where protein synthesis and therefore cell division have been inhibited in the presence of residual peptidoglycan synthesis (7).

The data in Fig. 6 and Table 1 for actinomycin D- and mitomycin C-treated cells seem to substantiate the membrane breathing or thickening hypothesis. After both treatments, the amount of glycerol incorporated is approximately the same in both cultures (Table 1); however, the actinomycin membranes thicken while the mitomycin membranes do not until after 30 min (Fig. 4). The discrepancy appears to be explained on the basis that mitomycin-inhibited cells divide for about the first 30 min, whereas the actinomycin inhibited cells do not. Thus in the mitomycin cells, the incorporated glycerol is put into new membrane surface area, and the thickness remains close to the control value, whereas in the nondividing actinomycin cells the glycerol incorporated apparently inflates existing membrane surfaces.

In the comparison of the kinetics for the relative increase in membrane thickening to the relative increase in amount of glycerol incorporated per cell (Fig. 6), it is obvious that the relative increase in membrane thickness is much less than the amount of glycerol accumulated. In considering this difference it should be noted that (i) a measurement of membrane thickness produces a two-dimensional value not related to mass, and (ii) even though the amount of glycerol incorporated per cell was calculated, an allowance was not made for changes in cell shape. Such changes in shape could have a dramatic effect on the amount of surface area per cell.

It may be unrealistic to expect that glycerol incorporation into membrane components would reflect rapid dynamic changes of the mesosomal pool (i) since the fraction of membrane lipid contained in the mesosomal membrane as compared to the cytoplasmic membrane as a whole is small, and (ii) since membranes may fluctuate in lipid-to-protein ratio on treatment as demonstrated by changes in membrane thickness.

As for the specificity of the glycerol label, it is known that in *S. faecalis* labeled glycerol remains as glycerol and is not converted into other precursors (12) and that virtually all the lipid found in this organism is membrane-associated (20). However, only 40 to 50% of the total glycerol label can be extracted in the chloroform-methanol phase (J. Dyckman, *personal communication*), suggesting that a sizable portion of the labeled glycerol may be incorporated into membrane-associated glycerol teichoic acid.

The question also arises as to how mesosomes are able to increase in size when protein synthesis is inhibited. Because of the small amount of membrane involved, little or no additional membrane protein may be required, and the new membrane may be formed by a rearrangement or dilution of existing membrane proteins or by the use of pretreatment membrane protein pools. Alternately, as suggested by Toennies for amino acid-starved cells, some preexisting cytoplasmic proteins may be converted into membrane proteins (20). However, as recently reviewed by Salton (15), in the case of chloramphenicol certain membrane proteins do continue to be synthesized in the presence of the inhibitor and could probably supply the amount of protein needed for the increases in mesosomal membrane observed here.

ACKNOWLEDGMENTS

We gratefully acknowledge the excellent technical assistance of M. P. O'Connor in electron microscopy and P. Washington in sample preparation and radioactive incorporation studies, and of M. Rosenhagen and E. Oldmixon, who worked on the early phases of this investigation. We also thank G. D. Shockman for his many productive suggestions and discussions during the course of this work.

This investigation was supported by National Science Foundation grant GB 31920. Public Health Service grant AI-05044 from the National Institute of Allergy and Infectious Diseases, and Temple University general research support grant.

LITERATURE CITED

1. Altenburg, B. C., J. C. Suit, and B. R. Brinkley. 1970. Ultrastructure of deoxyribonucleic acid-membrane associations in *Escherichia coli*. J. Bacteriol. 104:549–555.
2. Fielding, P., and F. Fox. 1970. Evidence for stable at-

tachment of DNA to membrane at the replication origin of *Escherichia coli*. Biochem. Biophys. Res. Commun. **41**:157-162.
3. Fuchs, E., and P. Hanawalt. 1970. Isolation and characterization of the DNA replication complex from *Escherichia coli*. J. Mol. Biol. **52**:301-322.
4. Ganesan, A. T., and J. Lederberg. 1965. A cell membrane bound fraction of bacterial DNA. Biochem. Biophys. Res. Commun. **18**:824-835.
5. Higgins, M. L., H. M. Pooley, and G. D. Shockman. 1971. Reinitiation of cell wall growth after threonine starvation of *Streptococcus faecalis*. J. Bacteriol. **105**: 1175-1183.
6. Higgins, M. L., and G. D. Shockman. 1970. Model for cell wall growth of *Streptococcus faecalis*. J. Bacteriol. **101**:643-648.
7. Higgins, M. L., and G. D. Shockman. 1970. Early changes in the ultrastructure of *Streptococcus faecalis* after amino acid starvation. J. Bacteriol. **103**:244-254.
8. Higgins, M. L., and G. D. Shockman. 1971. Procaryotic cell division with respect to wall and membranes. CRC Crit. Rev. Microbiol. **1**:29-72.
9. Jacob, F., S. Brenner, and F. Cuzin. 1963. On the regulation of DNA replication in bacteria. Cold Spring Harbor Symp. Quant. Biol. **28**:329-347.
10. Kahane, I., and S. Razin. 1969. Synthesis and turnover of membrane protein and lipid in *Mycoplasma laidlawii*. Biochim. Biophys. Acta **183**:79-89.
11. Mindich, L. 1970. Membrane synthesis in *Bacillus subtilis*. II. Integration of membrane proteins in the absence of lipid synthesis. J. Mol. Biol. **49**:433-439.
12. Pieringer, R. A., and R. T. Ambron. 1971. The metabolism of glyceride glycolipids. V. Identification of the membrane lipid formed from diglycosyl diglyceride in *Streptococcus faecalis* ATCC 9790 as an acylated derivative of glyceryl phosphoryl diglycosyl glycerol. J. Biol. Chem. **246**:4216-4225.
13. Roth, G. S., G. D. Shockman, and L. Daneo-Moore. 1971. Balanced macromolecular biosynthesis in "protoplasts" of *Streptococcus faecalis*. J. Bacteriol. **105**: 710-717.
14. Ryter, A. 1968. Association of the nucleus and the membrane of bacteria: a morphological study. Bacteriol. Rev. **32**:39-54.
15. Salton, R. J. 1971. Bacterial membranes. CRC Crit. Rev. Microbiol. **1**:161-197.
16. Smith, D. W., and P. C. Hanawalt. 1967. Properties of the growth point region of the bacterial chromosome. Biochim. Biophys. Acta **149**:519-531.
17. Sueoka, N., and W. G. Quin. 1968. Membrane attachment of the chromosome replication origin in *Bacillus subtilis*. Cold Spring Harbor Symp. Quant. Biol. **33**: 695-705.
18. Toennies, G., L. Iszard, N. B. Rogers, and G. D. Shockman. 1961. Cell multiplication studied with an electronic particle counter. J. Bacteriol. **82**:857-866.
19. Toennies, G., and G. D. Shockman. 1958. Growth chemistry of *Streptococcus faecalis*. Proc. 4th Int. Congr. Biochem., Vienna **13**:365-394.
20. Toennies, G., G. D. Shockman, and J. J. Kolb. 1963. Differential effects of amino acid deficiencies on bacterial cytochemistry. Biochemistry **2**:294-296.
21. Ziegler, R. J., and L. Daneo-Moore. 1971. Effects of essential amino acid starvation in *Streptococcus faecalis:* structural change in the 50*S* ribosomal subunit. J. Bacteriol. **105**:190-199.